Received: 22 December 2021 | Accepted: 15 June 2022

DOI: 10.1002/prp2.983

SHORT REPORT

Acute retigabine-induced effects on myelinated motor axons in amyotrophic lateral sclerosis

Boudewijn T. H. M. Sleutjes[1] | Diederik J. L. Stikvoort García[1] | Maria O. Kovalchuk[1] | Jules A. A. C. Heuberger[2] | Geert Jan Groeneveld[2] | Hessel Franssen[1] | Leonard H. van den Berg[1]

[1]Department of Neurology, Brain Center Utrecht, University Medical Center Utrecht, Utrecht, The Netherlands

[2]Center for Human Drug Research, Leiden, The Netherlands

Correspondence
Boudewijn T. H. M. Sleutjes, Department of Neurology, F02.230, University Medical Center Utrecht, P.O. Box 85500, 3508 GA, Utrecht, The Netherlands.
Email: b.sleutjes@umcutrecht.nl

Funding information
Biogen; EU Joint Programme - Neurodegenerative Disease Research, JPND; European Federation of Neurological Societies; Prinses Beatrix Spierfonds; Stichting ALS Nederland; the Netherlands Organization for Health Research and Development; Netherlands ALS Foundation

Abstract

Altered motor neuron excitability in patients with amyotrophic lateral sclerosis (ALS) has been suggested to be an early pathophysiological mechanism associated with motor neuron death. Compounds that affect membrane excitability may therefore have disease-modifying effects. Through which mechanism(s), these compounds modulate membrane excitability is mostly provided by preclinical studies, yet remains challenging to verify in clinical studies. Here, we investigated how retigabine affects human myelinated motor axons by applying computational modeling to interpret the complex excitability changes in a recent trial involving 18 ALS patients. Compared to baseline, the post-dose excitability differences were modeled well by a hyperpolarizing shift of the half-activation potential of slow potassium (K^+)-channels (till 2 mV). These findings verify that retigabine targets slow K^+-channel gating and highlight the usefulness of computational models. Further developments of this approach may facilitate the identification of early target engagement and ultimately aid selecting responders leading to more personalized treatment strategies.

KEYWORDS
axonal excitability, computational modeling, mechanism of action, target engagement

1 | INTRODUCTION

Amyotrophic lateral sclerosis (ALS) is a lethal neurodegenerative disease characterized by the progressive loss of central and peripheral motor neurons. Survival varies considerably because of differences in genetic and pathophysiological mechanisms.[1] Major challenges in the drug development process are the identification of these mechanisms and the development of sensitive techniques to detect pharmacological response and target engagement.[2]

A frequently observed mechanism in patients with ALS is motor neuron excitability.[3–5] It has been suggested that altered motor neuron excitability properties reflect an early pathophysiological step associated with motor neuron death.[6,7] Changes in excitability properties have been associated with shorter survival and a more

Abbreviations: ALS, amyotrophic lateral sclerosis; CMAPs, Compound muscle action potentials; HCN, hyperpolarization-activated cyclic nucleotide-gated; iPSC, induced pluripotent stem cell; SDTC, strength-duration time constant; SR, stimulus response.

aggressive disease course.[5,8] Hence, drugs that interact with membrane excitability may hold neuroprotective and disease-modifying properties.[9]

A compound that modulates motor neuron excitability is retigabine,[10,11] an anticonvulsant drug and potassium (K^+)-channel opener of which the molecular mechanisms are well-documented in preclinical studies.[12] Interestingly, in the context of drug repurposing, it was found to prolong survival of induced pluripotent stem cell (iPSC) derived motor neurons from ALS patients.[13] Recently, we demonstrated the acute effects of retigabine on motor axons of patients with ALS using nerve excitability testing.[14] Long-term exposure induced comparable motor axon excitability changes in patients with ALS.[15] Although challenging, verifying the mechanisms whereby compounds target human myelinated motor axons in vivo remains a vital part of translating preclinical to clinical findings. In this study, we performed an in-depth analysis of human nerve excitability recordings using computational modeling to provide insights into the modulatory mechanism of retigabine. Our findings may stimulate future applications and developments where such an integrated approach may eventually serve to verify early target engagement and potentially aid in identifying subjects who most likely respond to therapy.

2 | MATERIALS AND METHODS

2.1 | Study design and patient population

We obtained a subset of the motor nerve excitability recordings from a recent trial[14] in which 18 ALS patients participated (17 men, mean age 58.6 years, range 37–76). This subset involved recordings at baseline (pre-dose), 1.5 and 6 h post-dose on the day of retigabine administration (single dose, 300 mg). The patients gave written informed consent. The investigation was performed in accordance with the Declaration of Helsinki and was approved by the local medical ethical committee.

2.2 | Motor nerve excitability testing

The motor nerve excitability setup and protocol have been described extensively elsewhere.[14] Briefly, nerve excitability was assessed using Qtrac-S software (TRONDNF, Institute of Neurology, Queen Square). Non-polarizable surface electrodes (Red Dot, 3 M Health Care) were used for stimulation, with the cathode at the wrist over the median nerve, and the anode placed 10 cm proximal to the radial side of the forearm. Compound muscle action potentials (CMAPs) were recorded from the abductor pollicis brevis using surface electrodes in belly-tendon montage. In order to maintain a stable nerve temperature during the excitability tests, the median nerve was warmed by wrapping the forearm and hand in a warm water blanket through which water of 37°C flowed constantly (Norm-O-Temp & Maxi-therm lite infant hyper-hypothermia blanket for single patient use; Cincinnati Sub-Zero LLC) using a previously described warming procedure.[14,16]

To obtain multiple motor nerve excitability properties,[14] we applied a well-established excitability protocol, which consists of the stimulus response (SR) test to identify a target response (40% of the maximum CMAP amplitude), followed by the four main tests including the charge duration (Qt) relation (relation between stimulus charge [Q] and stimulus durations of 0.2, 0.4, 0.6, 0.8, and 1.0 ms) to estimate the strength-duration time constant (SDTC) and rheobase, the threshold electrotonus (time course of threshold changes before during and after a subthreshold depolarizing or hyperpolarizing conditioning current of 100-ms duration set at 20% and 40% of the current for an unconditioned target response), the current–voltage (I/V) relation (threshold changes to 200 ms conditioning currents varying from +50% depolarizing to −100% hyperpolarizing), and the recovery cycle (time course of threshold changes from 2 to 200 ms after a supramaximal stimulus).

2.3 | Computational modeling

To identify the biophysical basis that may underlie the retigabine-induced excitability changes, we fitted the recordings using a well-established computational model[17] of the human myelinated axon (MEMfit, QTRAC-P software, Institute of Neurology, London, UK). The model simulates the four excitability curves and incorporates the main membrane dynamics of nodal and internodal ion channels. The model includes nodal transient and persistent sodium (Na^+) permeability, the conductances of nodal and internodal slow and fast potassium (K^+) channels, internodal hyperpolarization-activated cyclic nucleotide-gated (HCN) channels, nodal and internodal leak channels, Barrett and Barrett (i.e., high-resistance pathways through the myelin sheath) conductance, as well as the gating kinetics of voltage-gated channels were allowed to vary. During optimization, the gating kinetics of voltage-gated channels located at the node and internode are coupled together. Temperature effects on ion channels are accounted for by Q_{10} values of the gating kinetics.[17] We assumed a small skin–nerve temperature gradient[18] by setting the temperature at 34°C, which was kept fixed during modeling.

First, we optimized the model to obtain the best fit with the baseline (pre-dose) excitability recordings of the 18 patients, such that the patients served as their own reference. The resulting baseline (pre-dose) model was then fitted to match the post-dose excitability recordings at 1.5 and 6 h. Given the preclinical evidence that retigabine targets slow K^+-channels, the two post-dose models were fitted by altering slow K^+-channel parameters one at a time to avoid over-parameterization of potential treatment effects. The procedure involved least-squares optimization, where the discrepancy between measured and simulated excitability curves was minimized using relative weights for each test: 0.5 (strength-duration), 2 (threshold electrotonus), 1 (recovery cycle),

and 1 (current-threshold).[19] The error was inversely weighted by the standard deviation at every measured threshold. The resting potential was not optimized during modeling, but it was allowed to vary in response to parameter changes. With this procedure, we obtained the most likely parameter that is targeted by retigabine and underlies the excitability difference between pre-dose and post-dose motor axons.

As we applied the computational model on excitability recordings from the day of retigabine administration, we provided some indications on the observed excitability changes on that day. For the extensive analysis based on the full dataset, we would like to refer to our recent trial.[14] We used a linear mixed effects model with the baseline (pre-dose) of the excitability indices as response, the individual excitability recordings as random intercept and equal weights to post-dose indices as fixed effect. Matlab (R2018a: The MathWorks) was used for statistical analyses. $p < .05$ was considered significant.

2.4 | Nomenclature of targets and ligands

Key protein targets and ligands in this article are hyperlinked to corresponding entries in http://www.guidetopharmacology.org, the common portal for data from the IUPHAR/BPS Guide to PHARMACOLOGY,[20] and are permanently archived in the Concise Guide to PHARMACOLOGY 2019/20.[21]

3 | RESULTS

3.1 | Pharmacokinetics and observed retigabine-induced excitability changes

The median highest plasma concentration for retigabine was 600 ng/ml (range: 271–997 ng/ml) with a median time to highest plasma concentration of 0.8 h (range: 0.5–4 h).

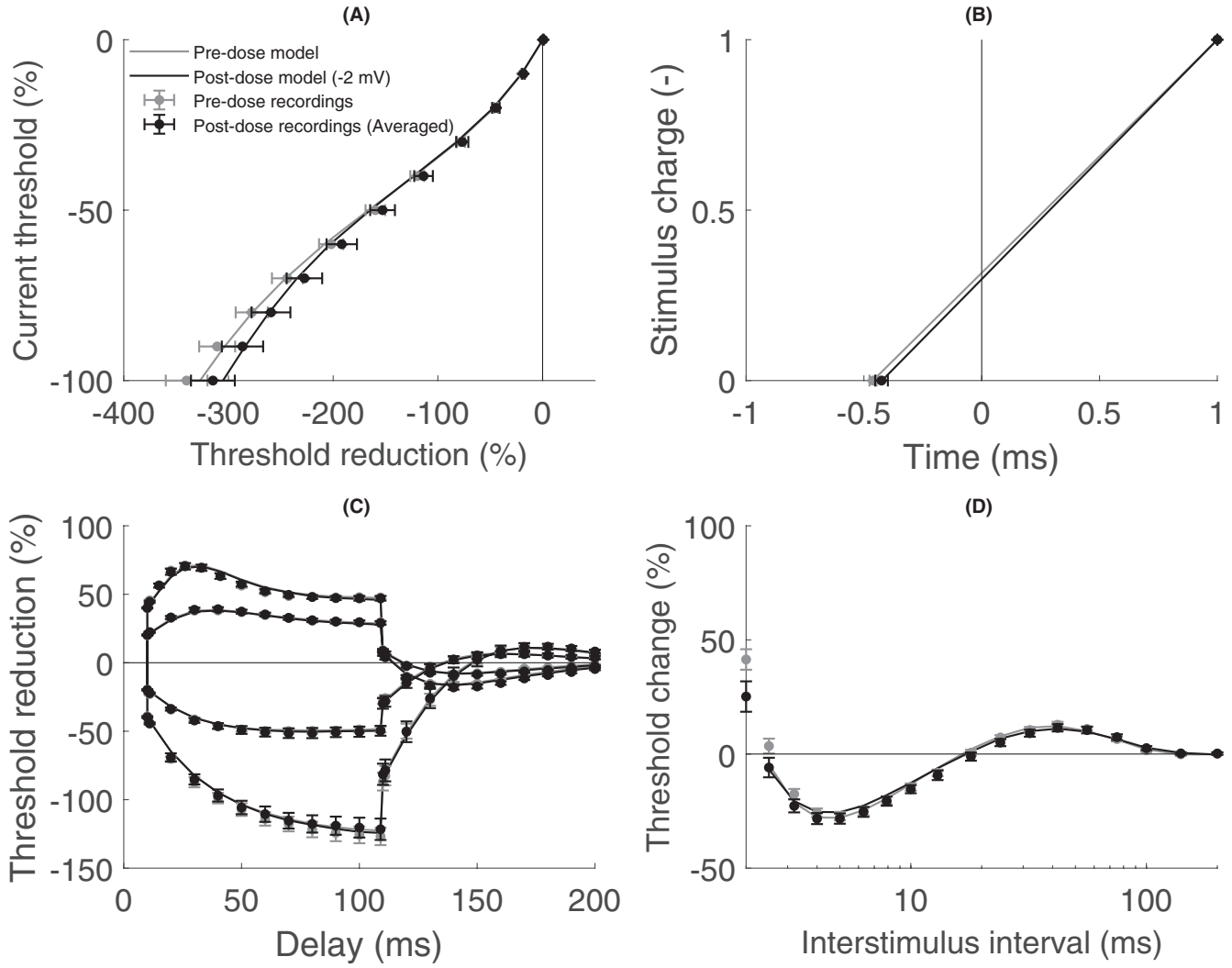

FIGURE 1 Recorded (dotted lines with SEM error bars) and modeled (solid lines) excitability curves at baseline (pre-dose, gray) and after retigabine administration (1.5 and 6 h averaged, black; −2 mV shift of half-activation potential of slow K^+-channels) with in (A) the hyperpolarizing part of the current/voltage relation, (B) strength-duration relation (normalized stimulus charge), (C) threshold electrotonus, and (D) the recovery cycle.

TABLE 1 Modeling results of the acute retigabine-induced effects on motor axons

		Pre-dose	Post-dose	
			1.5 h	6 h
Parameter	Description	Baseline model	Best single parameter (error reduction, %)	
Bas[a] (mV)	Half-activation potential of slow K^+-channels	−23.5	**−25.2 (30.3%)**	**−25.5 (42.6%)**
Aas[a] (ms^{-1})	Rate constant of slow K^+-channels	0.0058	0.0054 (16.8%)	0.0051 (30.5%)
GKsN (nS)	Maximal nodal slow K^+-conductance	40.5	41.1 (6.8%)	41.9 (3.4%)
ENR (mV)	Nodal resting membrane potential[a]	−81.1	−81.9[b]	−82.1[b]

Note: In bold = best single parameter followed by 2nd and 3rd best single parameter based on the error reductions.

[a]Half-activation potential (mV) and rate constant (ms^{-1}, at 34°C) of slow K^+-channels. The half-activation potential and rate constant for the transition rate α_s are only displayed, because the transition rates (α_s, β_s) are coupled in the model during optimization.

[b]The resting membrane potential is not optimized within the model, but hyperpolarizes as a consequence of hyperpolarization of the half-activation potential of slow K^+-channels.

Figure 1 illustrates the baseline (pre-dose) and averaged post-dose motor excitability recordings. Compared to baseline, retigabine shortened the strength-duration time constant (SDTC, Δ −0.04 ms, $p = .04$; 95% CI −0.07 to <−0.01 ms) and increased the rheobase (Δ0.6 mA, $p = .04$; 95% CI <0.1–1.2). The accommodation half-time prolonged (Δ2.5 ms, $p = .03$; 95% CI 0.2–4.7), and the depolarizing and hyperpolarizing threshold electrotonus (at 90–100 ms) showed no changes. The hyperpolarizing I/V at 100% increased (Δ23.7%, $p = .005$; 95% CI 7.7–39.8). The recovery cycle showed lower refractoriness at 2.5 ms (Δ −9.9%, $p = .002$; 95% CI −16 to −3.8%) and shorter relative refractory period (Δ −0.22 ms, $p = .002$; 95% CI −0.36 to −0.09).

3.2 | Biophysical basis of retigabine-induced excitability changes

Table 1 presents the optimized post-dose models using the baseline (pre-dose) model (Table S1). Hyperpolarizing shifts of the half-activation potential of slow K^+-channels produced the largest error reduction from baseline to the post-dose models (Δ1.7 mV, 30.3% error reduction at 1.5 h; Δ2 mV, 42.6% error reduction at 6 h). The second and third best fits involved a decelerated rate constant of slow K^+-channels and an increase in slow K^+-channel conductance, both at 1.5 and 6 h (Table 1). The changes in half-activation potential of slow K^+-channels hyperpolarized the resting membrane potential by 0.8 and 1.0 mV (Table 1). A hyperpolarizing shift of the half-activation potential and a decelerated rate constant of slow K^+-channels jointly resulted in an error reduction of 37.3% (Δ1.6 mV and 6.5% at 1.5 h) and 69% (Δ2.9 mV and 12.1% at 6 h). Modeled excitability curves for the baseline model and post-dose model (at 6 h) after a 2 mV hyperpolarizing shift of the half-activation potential of slow K^+-channels are illustrated in Figure 1.

3.3 | Altered slow K^+-channel gating and impact on open fraction at resting membrane potential

To determine how altered slow K^+-channel gating affects the fraction of open slow K^+-channels, we used the well-established steady-state relation.[22] Using the fitted model parameters (Table 1), a 2 mV hyperpolarizing shift in half-activation potential of slow K^+-channels (at 6 h) increased the fraction of open slow K^+-channels by approximately 10.2% at resting membrane potential (Figure 2A). Given the markedly higher slow K^+-conductances at the node compared to the internode,[23,24] the affected channels most likely involve nodal slow K^+-channels. Figure 2B shows a diagram of a myelinated axon highlighting the affected nodal slow K^+-channels.

4 | DISCUSSION

We showed that computational modeling verified retigabine's mechanism of action on motor neuron excitability in ALS patients. Obtaining such insights into the mechanisms by which compounds modulate membrane excitability is challenging in human subjects and, therefore often limited to preclinical models. Our findings may be significant, as compounds that modulate membrane excitability may have disease-modifying properties. Therefore, future applications and refinements of such sensitive techniques may be vital for assessing drug responses in phase 1 trials, which, in turn, may improve compound selection for phase 2 trials.

Our findings provide in vivo evidence that retigabine predominantly targets slow K^+-channel gating, evidence that—to date—had mainly been identified in preclinical studies.[10–12] Although human studies have shown effects of retigabine on the excitability of myelinated motor axons,[14,15] we have now provided quantitative support that modulation of slow K^+-channel gating underlies these effects, as previously speculated[14] based on preclinical studies.[10,11,25–28] Without a priori information, it would have been virtually impossible to interpret the complex set of altered excitability properties in our recent trial.[14] Computational modeling may, therefore, be key to the evaluation of compounds in nerve excitability studies. The timing of the excitability recordings in relation to the time to highest plasma concentration indicates that retigabine is rapidly absorbed and reaches myelinated motor axons quickly.

We are aware of the inherent uncertainty at various levels of the analyses, as described elsewhere.[29] Preclinical studies showed

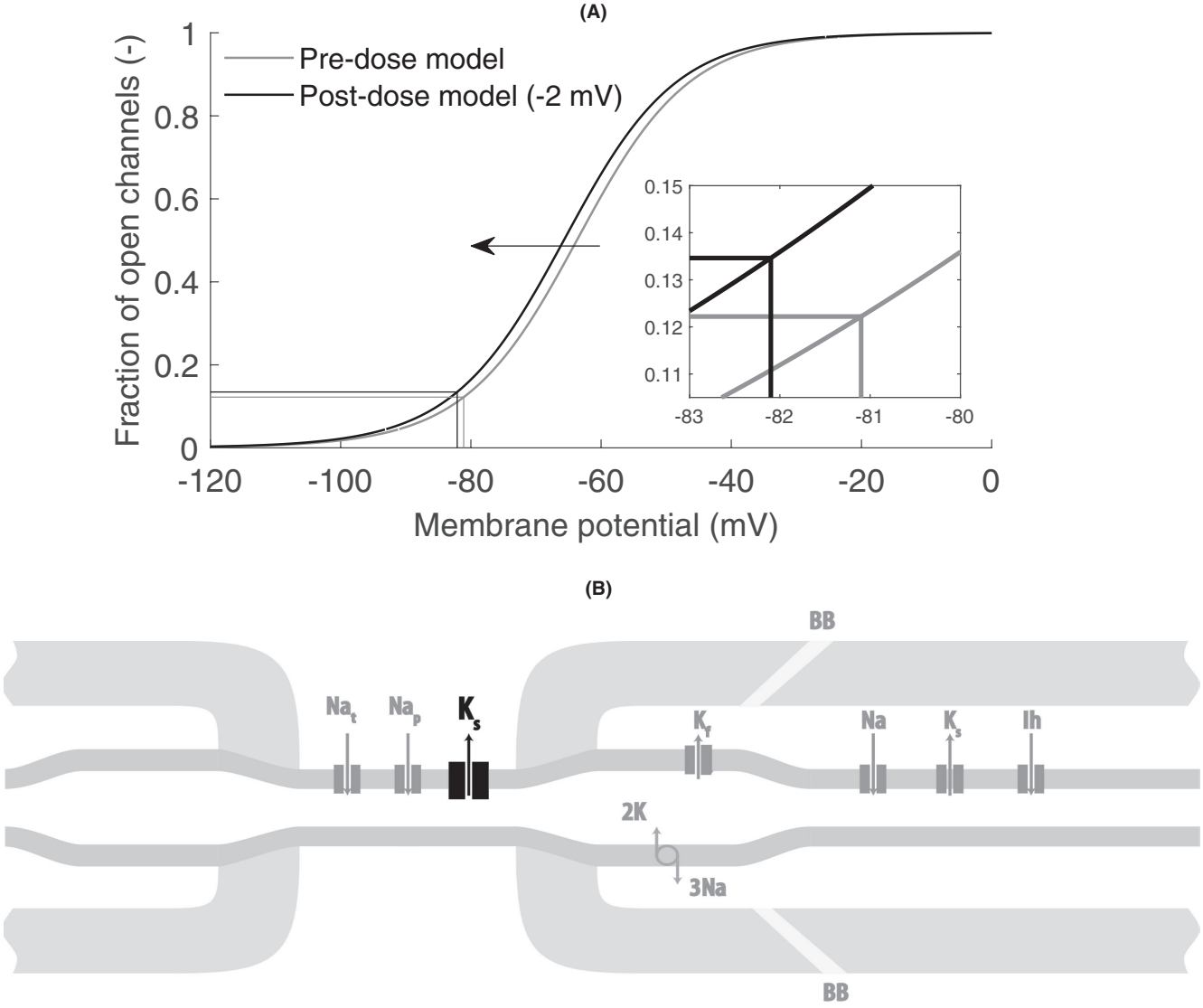

FIGURE 2 (A) Fraction of open slow K^+-channels based on the baseline (pre-dose) model (gray) and post-dose model (at 6 h) with a −2 mV shift of the half-activation potential. Inset in (A) shows region around resting membrane potential with an increased open fraction of 10.2% (100% [0.13463/0.1222–1]) for the post-dose model. In (B), a diagram of a myelinated axon in gray (modified from Franssen[34]): Na_t, transient Na^+; Na_p, persistent Na^+; K_s, slow K^+ with altered nodal gating kinetics in black (As slow K^+ channels are highly clustered in the node, reflected by the markedly higher nodal compared to internodal slow K^+-conductance, modeling results are therefore likely driven by nodal slow K^+-channels); K_f, fast K^+; I_h, hyperpolarization-activated cation (HCN) current; the Na^+/K^+ pump; BB, Barrett and Barrett resistance.

that nodal slow K^+-currents are mediated by KCNQ channels at the nodal domain, where retigabine can modulate these channels.[10,30,31] As slow K^+-channels are highly clustered at the node of Ranvier,[23,24] the modeling results, suggesting a hyperpolarizing shift of the half-activation potential, are therefore likely driven by nodal slow K^+-channels. Such modulation could induce stronger hyperpolarizing effects on depolarized axons, an effect previously linked to the potential difference with the K^+ equilibrium potential.[32,33] Modeling indicated further that also the rate constant may be involved, albeit to a lesser extent. These results confirm and extend the findings of our previous study,[14] although it should be noted that here we only used data from the day of retigabine administration. Additionally, the study involves a relative small number of patients, where a larger population may allow studying patient subgroups with specific pharmacokinetic characteristics in more detail. Advantageously, the computational model incorporates all excitability indices, including the affected and, equally importantly, the unaffected ones. For instance, rheobase, SDTC, and the hyperpolarizing part of the current–voltage were significantly affected, whereas threshold electrotonus remained largely unaffected. The modeling approach markedly reduces the ambiguities which would have arisen had we focused on altered excitability indices only.

In conclusion, the current findings indicate that clinical studies involving excitability recordings integrated with computational modeling could serve as a translational approach to verify the mechanism(s) of compounds that affect membrane excitability. Further

developments of our approach may ultimately delineate differences in drug responses between subjects, thus creating the possibility for timely distinction between responders and non-responders and personalized dosage levels.

AUTHORS' CONTRIBUTIONS

BTHMS and DJLSG wrote the manuscript. BTHMS, MK, JAACH, HF, GJG, and LHvdB designed the research. BTHMS, MK, and JAACH performed the research. BTHMS, MK, DJLSG, and JAACH analyzed the data.

FUNDING INFORMATION

BTHMS and DLJSG are funded by the Netherlands ALS Foundation, MK received grants from European Federation of Neurological Societies and Prinses Beatrix Spierfonds. HF received grants from Prinses Beatrix Spierfonds. LHvdB received funding from Netherlands ALS Foundation, the Netherlands Organization for Health Research and Development (Vici scheme), and the Netherlands Organization for Health Research and Development (SOPHIA, STRENGTH, ALS-CarE project), funded via the EU Joint Programme—Neurodegenerative Disease Research (JPND). Biogen funded the clinical trial from which the data of this work originates.

CONFLICT OF INTEREST

LHvdB served on the Scientific Advisory Board of Biogen, Cytokinetics, Prinses Beatrix Spierfonds and the Latran foundation. HF reports previous grants from Biogen and personal fees from Shire. JAACH and GJG report grants from Biogen.

DATA AVAILABILITY STATEMENT

The data that support the findings of this study are available from the corresponding author upon reasonable request.

ORCID

Boudewijn T. H. M. Sleutjes https://orcid.org/0000-0001-6618-3573
Jules A. A. C. Heuberger https://orcid.org/0000-0001-7202-5088

REFERENCES

1. van Es MA, Hardiman O, Chio A, et al. Amyotrophic lateral sclerosis. *Lancet*. 2017;390:2084-2098.
2. van Eijk RPA, Kliest T, CJ MD, et al. TRICALS: creating a highway toward a cure. *Amyotroph Lateral Scler Frontotemporal Degener*. 2020;21(7-8):496-501.
3. Bae JS, Simon NG, Menon P, Vucic S, Kiernan MC. The puzzling case of hyperexcitability in amyotrophic lateral sclerosis. *J Clin Neurol*. 2013;9:65-74.
4. Park SB, Kiernan MC, Vucic S. Axonal excitability in amyotrophic lateral sclerosis: axonal excitability in ALS. *Neurotherapeutics*. 2017;14:78-90.
5. Kanai K, Shibuya K, Sato Y, et al. Motor axonal excitability properties are strong predictors for survival in amyotrophic lateral sclerosis. *J Neurol Neurosurg Psychiatry*. 2012;83:734-738.
6. Gunes ZI, Kan VWY, Ye X, Liebscher S. Exciting complexity: the role of motor circuit elements in ALS pathophysiology. *Front Neurosci*. 2020;14:573.
7. Iwai Y, Shibuya K, Misawa S, et al. Axonal dysfunction precedes motor neuronal death in amyotrophic lateral sclerosis. *Plos One*. 2016;11:e0158596.
8. Shibuya K, Misawa S, Kimura H, et al. Increased motor axonal persistent sodium currents predict rapid functional declines in amyotrophic lateral sclerosis. *Neurol Clin Neurosci*. 2016;4:108-111.
9. Noto Y, Shibuya K, Vucic S, Kiernan MC. Novel therapies in development that inhibit motor neuron hyperexcitability in amyotrophic lateral sclerosis. *Expert Rev Neurother*. 2016;16:1147-1154.
10. Schwarz JR, Glassmeier G, Cooper EC, et al. KCNQ channels mediate IKs, a slow K+ current regulating excitability in the rat node of Ranvier. *J Physiol*. 2006;573:17-34.
11. Wickenden AD, Yu W, Zou A, Jegla T, Wagoner PK. Retigabine, a novel anti-convulsant, enhances activation of KCNQ2/Q3 potassium channels. *Mol Pharmacol*. 2000;58:591-600.
12. Redford KE, Abbott GW. KCNQ potassium channels as targets of botanical folk medicines. *Annu Rev Pharmacol Toxicol*. 2021;62:447-464.
13. Wainger BJ, Kiskinis E, Mellin C, et al. Intrinsic membrane hyperexcitability of amyotrophic lateral sclerosis patient-derived motor neurons. *Cell Rep*. 2014;7:1-11.
14. Kovalchuk MO, Heuberger JAAC, Sleutjes BTHM, et al. Acute effects of riluzole and retigabine on axonal excitability in patients with amyotrophic lateral sclerosis: a randomized, double-blind, placebo-controlled, crossover trial. *Clin Pharmacol Ther*. 2018;104:1136-1145.
15. Wainger BJ, Macklin EA, Vucic S, et al. Effect of ezogabine on cortical and spinal motor neuron excitability in amyotrophic lateral sclerosis: a randomized clinical trial. *JAMA Neurol*. 2021;78:186-196.
16. Kovalchuk MO, Franssen H, Scheijmans FEV, Van Schelven LJ, Van Den Berg LH, Sleutjes B. Warming nerves for excitability testing. *Muscle Nerve*. 2019;60:279-285.
17. Howells J, Trevillion L, Bostock H, Burke D. The voltage dependence of I(h) in human myelinated axons. *J Physiol*. 2012;590:1625-1640.
18. Howells J, Czesnik D, Trevillion L, Burke D. Excitability and the safety margin in human axons during hyperthermia. *J Physiol*. 2013;591:3063-3080.
19. Kovalchuk MO, Franssen H, van den Berg LH, van Schelven LJ, Sleutjes B. Excitability of motor and sensory axons in multifocal motor neuropathy. *Clin Neurophysiol*. 2020;131:2641-2650.
20. Harding SD, Sharman JL, Faccenda E, et al. The IUPHAR/BPS Guide to PHARMACOLOGY in 2018: updates and expansion to encompass the new guide to IMMUNOPHARMACOLOGY. *Nucleic Acids Res*. 2018;46:D1091-D1106.
21. Alexander SP, Mathie A, Peters JA, et al. THE CONCISE GUIDE TO PHARMACOLOGY 2019/20: ion channels. *Br J Pharmacol*. 2019;176(suppl 1):S142-S228.
22. Hodgkin AL, Huxley AF. A quantitative description of membrane current and its application to conduction and excitation in nerve. *J Physiol*. 1952;117:500-544.
23. Waxman SG, Ritchie JM. Molecular dissection of the myelinated axon. *Ann Neurol*. 1993;33:121-136.
24. Roper J, Schwarz JR. Heterogeneous distribution of fast and slow potassium channels in myelinated rat nerve fibres. *J Physiol*. 1989;416:93-110.
25. Corbin-Leftwich A, Mossadeq SM, Ha J, Ruchala I, Le AH, Villalba-Galea CA. Retigabine holds KV7 channels open and stabilizes the resting potential. *J Gen Physiol*. 2016;147:229-241.
26. Tatulian L, Brown DA. Effect of the KCNQ potassium channel opener retigabine on single KCNQ2/3 channels expressed in CHO cells. *J Physiol*. 2003;549:57-63.
27. Tatulian L, Delmas P, Abogadie FC, Brown DA. Activation of expressed KCNQ potassium currents and native neuronal M-type potassium currents by the anti-convulsant drug retigabine. *J Neurosci*. 2001;21:5535-5545.

28. Gunthorpe MJ, Large CH, Sankar R. The mechanism of action of retigabine (ezogabine), a first-in-class K+ channel opener for the treatment of epilepsy. *Epilepsia*. 2012;53:412-424.
29. Mirams GR, Pathmanathan P, Gray RA, Challenor P, Clayton RH. Uncertainty and variability in computational and mathematical models of cardiac physiology. *J Physiol*. 2016;594:6833-6847.
30. Pan Z, Kao T, Horvath Z, et al. A common ankyrin-G-based mechanism retains KCNQ and NaV channels at electrically active domains of the axon. *J Neurosci*. 2006;26:2599-2613.
31. Devaux JJ, Kleopa KA, Cooper EC, Scherer SS. KCNQ2 is a nodal K+ channel. *J Neurosci*. 2004;24:1236-1244.
32. Lang PM, Fleckenstein J, Passmore GM, Brown DA, Grafe P. Retigabine reduces the excitability of unmyelinated peripheral human axons. *Neuropharmacology*. 2008;54:1271-1278.
33. Rundfeldt C. The new anticonvulsant retigabine (D-23129) acts as an opener of K+ channels in neuronal cells. *Eur J Pharmacol*. 1997;336:243-249.
34. Franssen H. The node of Ranvier in multifocal motor neuropathy. *J Clin Immunol*. 2014;34(suppl 1):S105-S111.

SUPPORTING INFORMATION

Additional supporting information can be found online in the Supporting Information section at the end of this article.

How to cite this article: Sleutjes BTH, Stikvoort García DJL, Kovalchuk MO, et al. Acute retigabine-induced effects on myelinated motor axons in amyotrophic lateral sclerosis. *Pharmacol Res Perspect*. 2022;10:e00983. doi: 10.1002/prp2.983